



## Correlation of Inflow Velocity Ratio Detected by Phase Contrast Magnetic Resonance Angiography with the Bleb Color of Unruptured Intracranial Aneurysms

Hiroki Uchikawa<sup>1,3</sup>, Taichi Kin<sup>1</sup>, Yasuhiro Takeda<sup>1</sup>, Tsukasa Koike<sup>1</sup>, Satoshi Kiyofuji<sup>1</sup>, Satoshi Koizumi<sup>1</sup>, Taketo Shiode<sup>1</sup>, Yuichi Suzuki<sup>2</sup>, Satoru Miyawaki<sup>1</sup>, Hirofumi Nakatomi<sup>1</sup>, Akitake Mukasa<sup>3</sup>, Nobuhito Saito<sup>1</sup>

**BACKGROUND:** Intraoperative rupture is the most fatal and catastrophic complication of surgery for unruptured intracranial aneurysms (UIAs); thus, it is extremely useful to predict reddish and thin-walled regions of the UIA before surgery. Although several studies have reported a relationship between the hemodynamic characteristics and intracranial aneurysm wall thickness, a consistent opinion is lacking. We aimed to investigate the relationship between objectively and quantitatively evaluated bleb wall color and hemodynamic characteristics using phase-contrast magnetic resonance angiography (PC-MRA).

**METHODS:** Ten patients diagnosed with UIA who underwent surgical clipping and preoperative magnetic resonance imaging along with PC-MRA were included in this study. Bleb wall color was evaluated from an intraoperative video. Based on the Red (R), Green, and Blue values, bleb wall redness (modified R value; mR) was calculated and compared with the hemodynamic characteristics obtained from PC-MRA.

**RESULTS:** The wall redness distribution of 18 blebs in 11 UIAs in 10 patients was analyzed. Bleb/neck inflow velocity ratio (Vb/Va:  $r = 0.66$ ,  $P = 0.003$ ) strongly correlated with mR,

whereas bleb/neck inflow rate ratio ( $r = 0.58$ ,  $P = 0.012$ ) correlated moderately. Multivariate regression analysis revealed that only Vb/Va ( $P = 0.017$ ) significantly correlated with mR. There was no correlation between wall shear stress and mR.

**CONCLUSIONS:** The bleb redness of UIAs and Vb/Va, calculated using PC-MRA, showed a significantly greater correlation. Thus, it is possible to predict bleb thickness noninvasively before surgery. This will facilitate more detailed pre- and intraoperative strategies for clipping and coiling for safe surgery.

### INTRODUCTION

Neurosurgeons take great efforts to avoid the intraoperative rupture of aneurysms, which is the most fatal and catastrophic complication of surgery for unruptured intracranial aneurysms (UIAs). Translucent aneurysms are reported to be at risk of intraoperative rupture; therefore, it is extremely important, yet difficult, to detect reddish and thin-walled regions (TIWRs) of UIA before surgery.<sup>1</sup> Although several studies have reported a

### Key words

- Bleb
- Inflow velocity ratio
- Phase contrast magnetic resonance angiography
- Unruptured intracranial aneurysm
- Wall thickness

### Abbreviations and Acronyms

- 3D:** 3-dimensional
- CFD:** Computational fluid dynamics
- mR:** Modified R value
- MRI:** Magnetic resonance imaging
- PC-MRA:** Phase-contrast magnetic resonance angiography
- Qa:** Inflow rate of the aneurysm
- Qb:** Inflow rate of the bleb
- Qb/Qa:** Bleb/neck inflow rate ratio
- RGB:** Baseline red, green, and blue
- RRT:** Relative residence time
- TIWRs:** Thin-walled regions
- TOF:** Time-of-flight

**UIAs:** Unruptured intracranial aneurysms

**Va:** Inflow velocity of the aneurysm

**Vb:** Inflow velocity of the bleb

**Vb/Va:** Bleb/neck inflow velocity ratio

**WSS:** Wall shear stress

From the Departments of <sup>1</sup>Neurosurgery and <sup>2</sup>Radiology, University of Tokyo, Tokyo; and <sup>3</sup>Department of Neurosurgery, Graduate School of Medical Sciences, Kumamoto University, Kumamoto, Japan

To whom correspondence should be addressed: Taichi Kin, M.D., Ph.D.  
[E-mail: tkin-ty@umin.ac.jp]

Citation: *World Neurosurg.* X (2021) 10:100098.  
<https://doi.org/10.1016/j.wnsx.2021.100098>

Journal homepage: [www.journals.elsevier.com/world-neurosurgery-x](http://www.journals.elsevier.com/world-neurosurgery-x)

Available online: [www.sciencedirect.com](http://www.sciencedirect.com)

2590-1397/© 2021 The Authors. Published by Elsevier Inc. This is an open access article under the CC BY-NC-ND license (<http://creativecommons.org/licenses/by-nc-nd/4.0/>).

relationship between hemodynamic characteristics and intracranial aneurysm wall thickness,<sup>2–7</sup> there is no consensus. Some studies report that TIWRs were associated with low wall shear stress (WSS),<sup>4</sup> whereas some report an association with high WSS.<sup>2,7</sup> Most of these studies were analyzed by computational fluid dynamics (CFD), although a few studies report using phase-contrast magnetic resonance angiography (PC-MRA).<sup>2,8,9</sup> To the best of our knowledge, no study has compared the intraoperative appearance of the aneurysmal wall and PC-MRA analysis. In addition, no study has objectively evaluated the color or thickness of the aneurysm walls. Given the previous qualitative evaluation, bias may exist. Thus, this study aimed to compare the hemodynamic characteristics of UIA using PC-MRA and quantitative bleb redness, with the intraoperative findings obtained during microscopic surgery.

## METHODS

### Ethical Approval

All procedures involving human participants were in accordance with the ethical standards of the institutional research committee and with the 1964 Helsinki Declaration and its later amendments. This study was approved by the institutional ethical committee, and informed consent was obtained from all individual participants before the commencement of the study.

### Patient Selection

From December 2018 to November 2019, patients diagnosed with UIA who underwent surgical clipping were included. Preoperative magnetic resonance imaging (MRI) with PC-MRA was performed, and hemodynamic parameters were analyzed. Patients who underwent both a 3-dimensional (3D) PC-MRA for flow velocity vector data and a 3D time-of-flight (TOF)-MRA for the shape of the vessel walls before craniotomy for UIA clipping were included. Thrombosed aneurysms were excluded because it was difficult to detect the aneurysm shape on TOF-MRA. Completely round aneurysms without a bleb also were excluded because it was difficult to set a plane at the root of the blebs. Case exclusion was performed independently of the flow analysis results.

### Imaging Sequences

MRI scans were obtained with a 3-T scanner (MAGNETOM Skyra; Siemens, Erlangen, Germany) with a slew rate of 200 T/m/s. We used a 20-channel head array coil. The imaging parameters for the 3D TOF-MRA were as follows: repetition time/echo time/number of excitations, 36 milliseconds/3.6 milliseconds/1; flip angle, 18°; field of view, 210 × 240 mm; matrix, 450210 × 512; voxel size, 0.47210 × 0.47210 × 0.5 mm; bandwidth, 305 Hz/pixel; scanning time, 8 minutes, 47 seconds. The imaging parameters for the 3D PC-MRA were as follows: repetition time/echo time/number of excitations, 37.7 milliseconds/5.46 milliseconds/2; flip angle, 10°; field of view, 199210 × 220 mm; matrix, 348210 × 384; voxel size, 0.57210 × 0.57210 × 1 mm; bandwidth, 365 Hz/pixel; scanning time 7 minutes, 28 seconds. The velocity encoding rate was 100–150 cm/s in 3 directions (anterior–posterior, right–left, and superior–inferior).

### Image Processing

The overview of image processing is shown in **Figure 1**. The shape of the vessel wall and the blood flow vector were created from

TOF-MRA and PC-MRA, respectively. Raw data were transferred to the image-processing software, Avizo (Thermo Fisher Scientific, Waltham, Massachusetts, USA). TOF-MRA was transformed with affine registration to the magnitude data of PC-MRA by the normalized mutual information method; a preliminary study was referred to in detail.<sup>10</sup> Thus, the position and posture of TOF-MRA and PC-MRA matched. The threshold was set by the full-width half-maximum criterion,<sup>11</sup> and the vessel wall was created by the surface rendering method. 3D phase data of PC-MRA were cropped in each direction by the vessel wall. The obtained data were transferred to the analysis software, IV-FLOW (Maxnet Co. Ltd., Tokyo, Japan). WSS was calculated according to the formula described in the next paragraph. The blebs visible in the intraoperative video were segmented, and the mean, maximum, and minimum WSS were analyzed. In addition, the inflow rate (Qb), mean inflow velocity (Vb), and area of the blebs were measured. To evaluate the local blood flow, the plane was set at the root of the bleb (**Figure 1**). Furthermore, the inflow rate (Qa) and inflow velocity (Va) entering the neck of the aneurysm were measured, and the correlation was verified using the ratios based on them (Qb/Qa, Vb/Va). The inlet of the aneurysms and blebs were identified by the neurosurgeon and displayed as a plane, set with reference to a plane approximating the polygon, using the iterative closest point algorithm.

### WSS Calculation

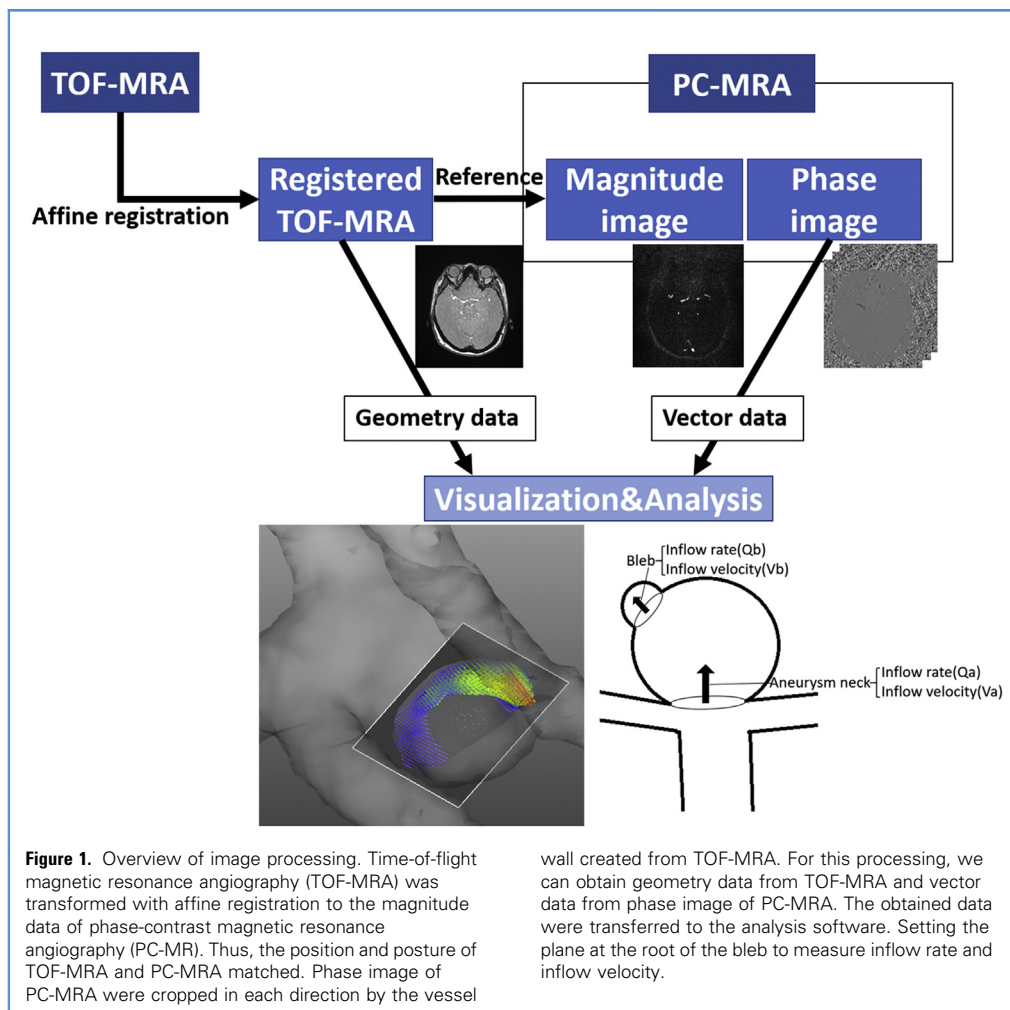
WSS was calculated by Smoothed Particle Hydrodynamics in analysis software.<sup>12</sup> The formula is detailed in the **Supplementary Methods**.

### Wall Color Quantification

OPMI PENTERO 900 (Carl Zeiss, Oberkochen, Germany) and OME-9000 (OLYMPUS, Tokyo, Japan) were used as surgical microscopes. First, the white balance of the microscope was adjusted, and baseline red, green, and blue (RGB) values were set. Then, the aneurysm bleb was clearly identified in the intraoperative video. Before color analysis using the captured image, the white balance was adjusted again to eliminate the effect of light on RGB values, using the commercial software Photoshop Elements (Adobe Inc., San Jose, California, USA). The image was decomposed into R, G, and B channels in the RGB color model using Avizo. The bleb was segmented in the intraoperative video. Then, the mean R, G, and B values for that region were calculated. To create a scale from 0 (white) to 255 (red), we calculated the average of G and B values and subtracted them from 255; this subtraction signified black and white inversion. In this manner, the modified R value (mR) was calculated to quantify bleb redness (**Figure 2**). The formula used was  $mR = 255 - (G + B)/2$ .

### Statistical Analysis

All statistical analyses were conducted using Easy R (Jichi Medical University Saitama Medical Center, Saitama, Japan). Spearman's rank correlation coefficient was used, and a P value <0.05 was considered statistically significant.<sup>13</sup> Factors showing significant correlation with mR, detected by univariate correlation analysis, were subsequently analyzed by multiple regression analysis.



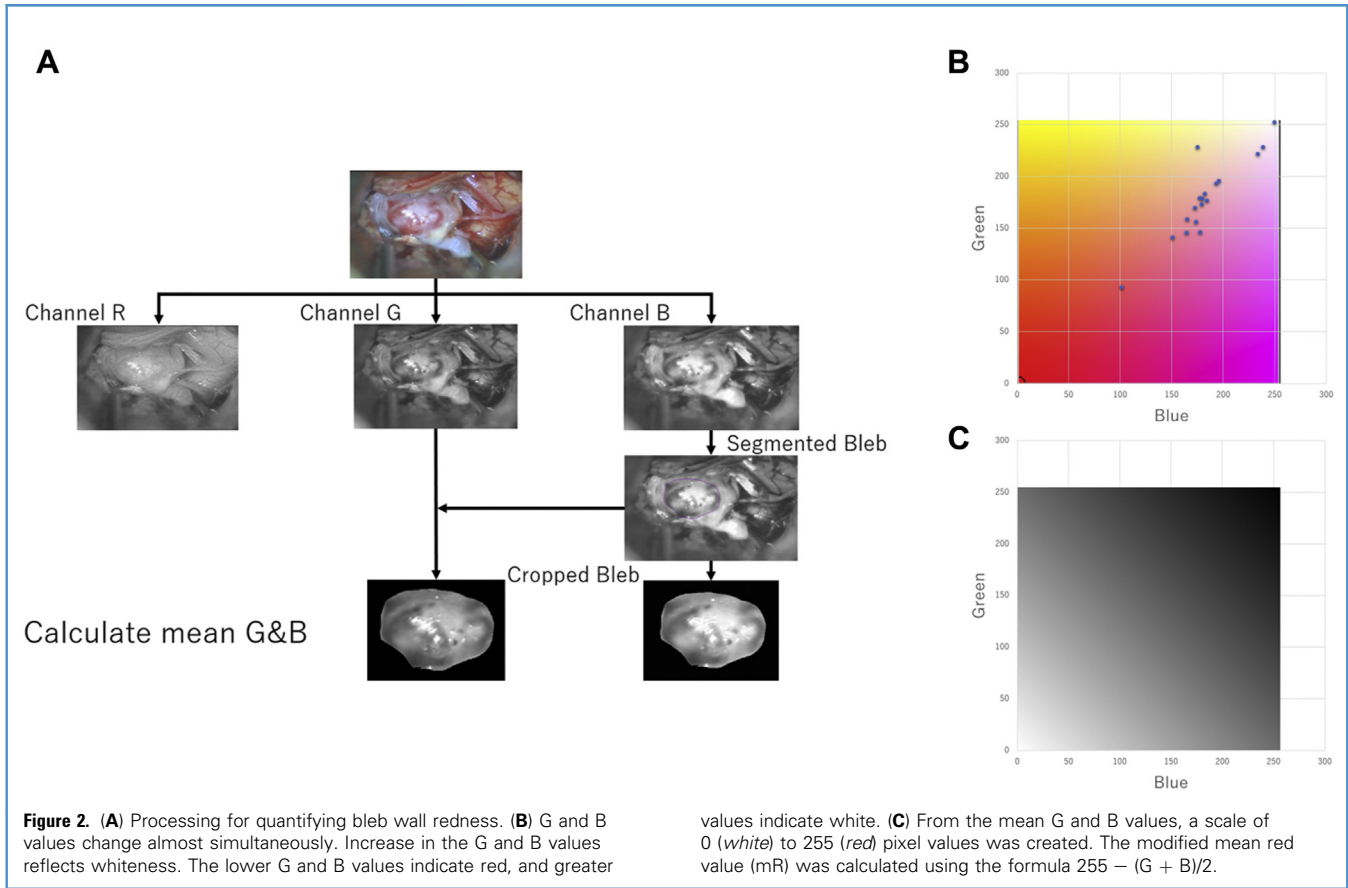
## RESULTS

Thirteen patients met the inclusion criteria, but one patient without a bleb, one with thrombosed aneurysm, and another without an intraoperative video were excluded. Finally, 10 patients were included, and the wall redness distribution of 18 blebs in 11 unruptured saccular aneurysms were analyzed (Table 1). The mean patient age was  $64.3 \pm 6.1$  years, and the mean aneurysmal size was  $7.5 \pm 1.7$  mm. There were 4 aneurysms in the middle cerebral artery, 4 in the internal carotid artery, 2 in the anterior communicating artery, and one in the distal anterior cerebral artery.

Table 2 shows the correlation of bleb redness and hemodynamic parameters. Bleb/neck inflow velocity ratio ( $V_b/V_a$ :  $r = 0.66$ ,  $P = 0.003$ ) was strongly related to mR (Figure 3), and bleb/neck inflow rate ratio ( $Q_b/Q_a$ :  $r = 0.58$ ,  $P = 0.012$ ) was moderately related. No correlation was found between the mean, maximum, and minimum WSS with mR. Multivariate regression analysis revealed that only  $V_b/V_a$  (regression coefficient = 109.3, 95% confidence interval 22.5–196.1;  $P = 0.017$ ) correlated with mR (Table 3). A representative case is shown in Figure 4.

## DISCUSSION

In our study,  $Q_b$  and  $V_b$  correlated weakly with mR. Since the bleb inflow rate and velocity varied greatly depending on the case, we calculated the inflow rate ratio ( $Q_b/Q_a$ ) and velocity ratio ( $V_b/V_a$ ) based on the neck inflow rate and velocity. Consequently,  $Q_b/Q_a$  and  $V_b/V_a$  significantly correlated with mR; in particular,  $V_b/V_a$  correlated strongly.  $V_b/V_a$  could be a useful parameter to predict bleb redness. High  $V_b/V_a$  indicates that the neck inflow goes directly into the bleb, such as an inflow jet. The impingement zone of the inflow jet is known as the high-pressure area, which tends to form blebs,<sup>14</sup> and is related to TIWRs.<sup>15,16</sup> Therefore, velocity reflects inflow jet more precisely than flow rate, showing a strong correlation with bleb wall thinning. On the contrary, a low  $V_b/V_a$  indicates that the neck inflow is weakened and stagnant near the bleb wall. Relative residence time (RRT) prolongation has been reported to be associated with atherosclerosis of the aneurysm wall, which corresponds to stagnation of blood flow.<sup>17</sup> The fact that the inflow velocity of the bleb is weakened compared with that of the aneurysmal neck signifies stagnation of blood flow, similar to that in



prolonged RRT. Thus, we assumed that measuring the inflow rate and velocity to the bleb and neck could indicate the thickness of the bleb wall unitarily.

In this study, WSS did not correlate with the color of the bleb wall. The color of the bleb wall could not be evaluated unitarily, possibly because there are different mechanisms for low and high WSS.<sup>18</sup> The

**Table 1. Patient Characteristics**

Patient	Age, years	Sex	Aneurysm	Location	Size, mm	Number of Blebs
1	65	F	1	Distal ACA	10.7	2
2	68	F	2	MCA	7.4	2
3	69	F	3	MCA	6.4	3
4	52	F	4	ICA	7.2	3
5	71	M	5	MCA	6.5	1
6	64	F	6	Acom	6.6	1
7	73	F	7	ICA	7.1	1
			8	MCA	5.1	1
8	60	F	9	ICA	6.3	1
9	63	F	10	ICA	10.7	2
10	58	M	11	Acom	8.0	1

F, female; ACA, anterior cerebral artery; MCA, middle cerebral artery; ICA, internal carotid artery; M, male; Acom, anterior communicating artery.

**Table 2.** Correlations of Bleb Redness with Clinical Variables and Hemodynamic Parameters

	Mean ± SD	Correlation (r)	P Value
modified R value, mR	73.9 ± 35.0		
Age, years	64.3 ± 6.1	−0.086*	0.74*
Aneurysm size, mm	7.5 ± 1.7	−0.056*	0.82*
Cross section of bleb, mm <sup>2</sup>	12.5 ± 6.0	0.12*	0.65*
Bleb height, mm	2.0 ± 0.66	−0.07*	0.78*
Mean WSS, Pa	1.33 ± 1.09	0.30*	0.23*
Maximum WSS, Pa	3.23 ± 2.49	0.41*	0.09*
Minimum WSS, Pa	0.65 ± 0.69	0.30*	0.22*
Bleb inflow rate, Q <sub>b</sub> , cm <sup>3</sup> /s	3.51 ± 3.08	0.47*	0.049*
Bleb inflow velocity, V <sub>b</sub> , cm/s	41.0 ± 23.3	0.48*	0.046*
Bleb inflow area, mm <sup>2</sup>	8.00 ± 4.00	0.28*	0.27*
Bleb/neck inflow rate ratio, Q <sub>b</sub> /Q <sub>a</sub>	0.48 ± 0.34	0.58*	0.012*
Bleb/neck inflow velocity ratio, V <sub>b</sub> /V <sub>a</sub>	0.56 ± 0.21	0.66*	0.0028*

SD, standard deviation; mR, modified red value; WSS, wall shear stress.  
\*Spearman's rank correlation coefficient.

magnitude of WSS correlated between CFD and PC-MRA, and differences in image modalities had little effect on results.<sup>8,19</sup>

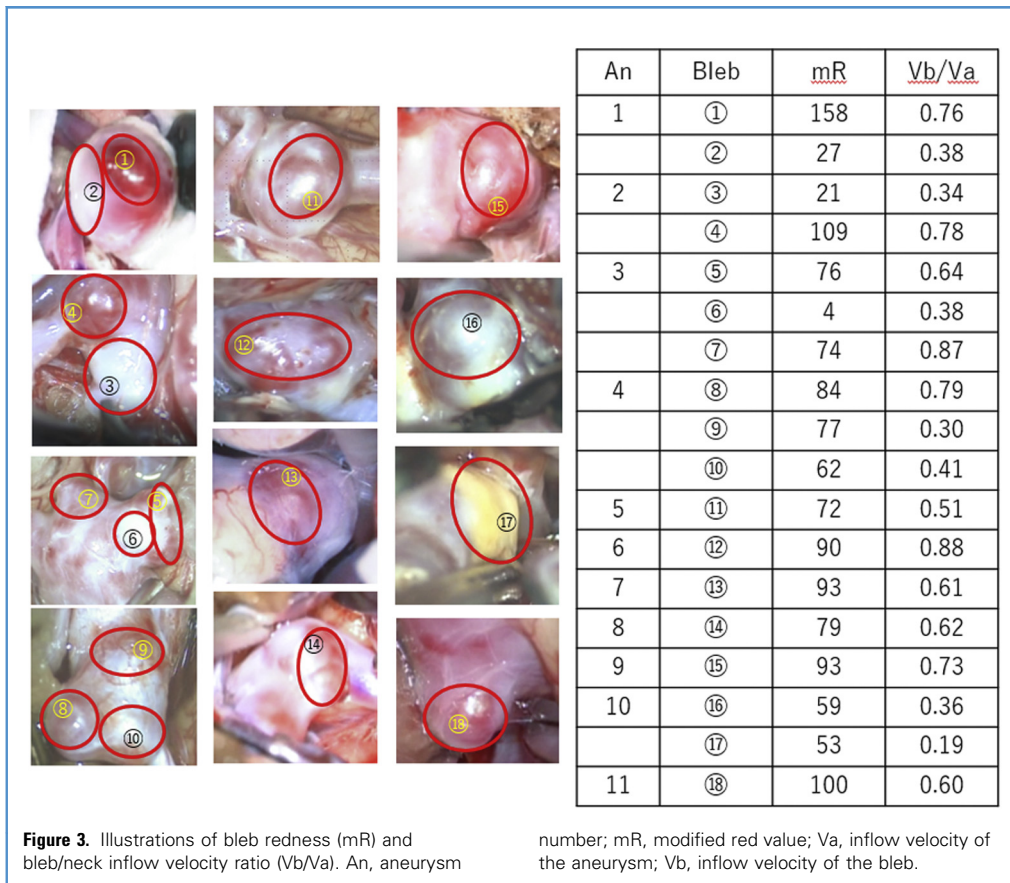
To the best of our knowledge, this study is the first report demonstrating a correlation between hemodynamic characteristics and intraoperative findings of the bleb wall using PC-MRA, highlighting the usefulness of the new parameter to predict bleb wall redness, independent of well-known parameters such as WSS, and evaluating bleb wall redness quantitatively and objectively.

Earlier fluid analysis of intracranial aneurysms had several problems. The first problem is related with the heterogeneity and inaccuracy of CFD. Various temporary parameter settings are needed for analysis with CFD, but the methods differ for each facility, sometimes leading to different results.<sup>20,21</sup> In addition, it might not reflect accurate hemodynamics because problems, such as blood-wall interaction, have not been technically solved.<sup>22</sup> In addition, few studies have analyzed the hemodynamics of intracranial aneurysms using PC-MRA<sup>2,8</sup>; conversely, most previous papers used CFD.<sup>3–7</sup> Thus, this is the first paper comparing the actual intraoperative findings of UIA with hemodynamic characteristics using PC-MRA. PC-MRA is an imaging method that can directly extract the direction and velocity of blood flow in situ, and it eliminates the need for most parameter settings, reducing the differences between facilities.

The second problem is associated with setting parameters. Several reports have compared hemodynamic characteristics with intraoperative findings during craniotomy for intracranial aneurysms.<sup>3–7</sup> Some studies report that TIWRs had low WSS,<sup>4,23</sup> whereas some reported that TIWRs had high WSS.<sup>2,7</sup> Thus, there is no consensus. It is believed that high and low WSS represent different mechanisms,<sup>18</sup> and it would be difficult to evaluate the two in the same field. Suzuki et al. reported that TIWRs can be detected by pressure difference.<sup>15</sup> Sugiyama

et al.<sup>17</sup> reported, with reference to atherosclerosis, that sites with prolonged RRT were associated with TIWRs. However, these parameters cannot detect both thinning and thickening. Since discussing the aneurysmal wall thickness with WSS alone and previously reported parameters has limitations, we decided to measure the local blood flow of the bleb, in addition to WSS.

The third problem is the method of evaluating the aneurysm wall. There are some methods to evaluate aneurysm wall thickness quantitatively. One is to cut the aneurysm walls and measure them directly under a microscope. However, in clinical practice, this method is not recommended due to the risk of bleeding. The evaluation of the aneurysm wall should, thus, be performed indirectly. The other methods are referencing the aneurysm wall redness or vessel wall imaging with MRI. A study evaluated the aneurysm wall thickness by vessel wall imaging with 7-T MRI,<sup>2</sup> but as the result was not compared with intraoperative findings, the credibility of vessel wall imaging remains unclear. In previous studies, the evaluation of aneurysm wall color was only a qualitative assessment that classified the aneurysm wall into 2–5 colors<sup>5,15,24</sup> and no quantitative assessment was conducted. A more objective and quantitative evaluation is required. Translucent aneurysms, whose dome showed reddish pigmentation, were reported to be at risk of intraoperative rupture.<sup>1</sup> If it were possible to predict the redness of the aneurysm wall preoperatively, it would greatly affect the surgical strategy to avoid intraoperative rupture. In case of endovascular coil embolization, wherein we cannot directly observe the aneurysm wall color, it is useful to assume thin blebs in the aneurysm wall before treatment, because it greatly affects the preoperative and intraoperative strategies such as the guidance of the microcatheter, order of the embolization compartment, and the force used to push the coil.



Hence, we devised the aforementioned formula based on the RGB value to evaluate the aneurysm wall redness objectively and quantitatively. In aneurysm walls, the part that seems to be thin is red, and the part that seems to have arteriosclerosis is white (or yellow). In the RGB color model, both red and white have high R values; we cannot distinguish between them. Therefore, we focused on the G and B values, as they changed almost simultaneously (Figure 2B), and there was no green or blue color on the aneurysm wall. This means that an increase in the G and B values reflects whiteness. If the R value is not taken into account, the lower G

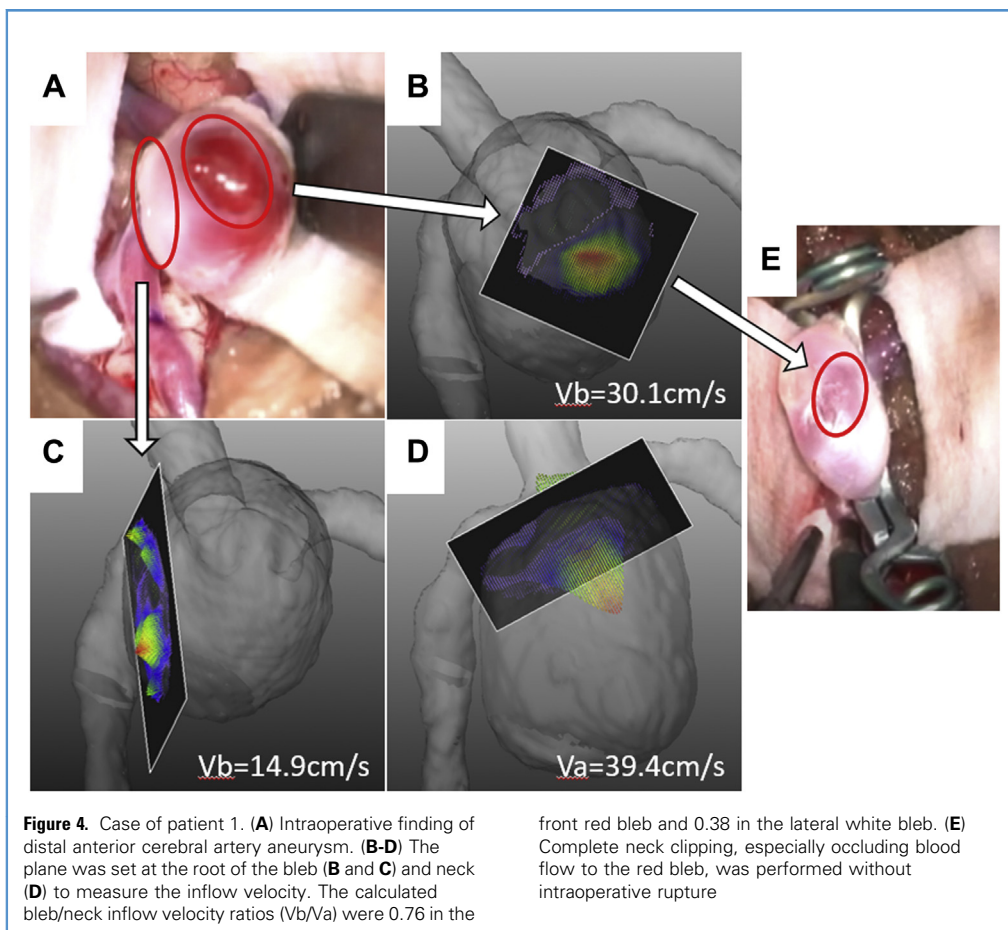
and B values indicate red, and higher indicate white. By calculating the average of the G and B values and subtracting that value from 255, a scale from 0 (white) to 255 (red) pixel values was created (Figure 2C). Then, the average mean G and B values of the bleb were applied, and the mR was calculated, so that the redness of the bleb could be quantitatively and objectively evaluated.

Our study has several limitations. First, it is not clear whether bleb redness directly reflects the measured wall thickness proportionally. As neurosurgeons, we observe that red bleb walls tend to be thin and rupture easily during surgery, which has been reported previously.<sup>1</sup> Therefore, the current method of color evaluation is not perfect. For example, yellow walls, which have atherosclerosis and are thicker than white walls, have larger mR than white walls, according to our formula. However, the yellow wall was quite similar to the white in terms of mR. Moreover, the angle of the microscope light could change the RGB value slightly, due to the change in the brightness of the surgical field. We tried to standardize the reference RGB value by adjusting the white balance of the microscope and eliminated the influence of light by adjusting the white balance of the image again, before RGB analysis. Furthermore, the RGB value could change during the process of converting analog data to digital data. However, its effect would be limited, since spherical and chromatic aberrations of recent microscopes are very small.<sup>25</sup>

**Table 3.** Multiple Regression Analysis of Bleb Redness and Hemodynamic Parameters

	Regression Coefficient	95% CI	P Value
Qb/Qa	-1.96	-57.0 to 53.1	0.94
Vb/Va	109.3	22.5 to 196.1	0.017
Adjusted R-squared	0.35		

CI, confidence interval; Qb/Qa, bleb/neck inflow rate ratio; Vb/Va, bleb/neck inflow velocity ratio.



Second, the position and posture of PC-MRA, TOF-MRA, and intraoperative findings may be slightly different from each other. If we evaluate only a part of the characteristic wall color, it tends to increase susceptibility to selection bias and position and posture shift among modalities. In this study, the bleb was used as a landmark to reduce the shift among modalities, and the evaluation was made with the average RGB value of the entire bleb for objective analysis.

Third, this was a retrospective study with a small sample size. In the multiple regression analysis, the result has very wide 95% confidence interval because of it. More samples are desirable for more accurate statistical analysis.

Presently, wall thickness measurements by vessel wall MRI are not accurate or reliable.<sup>26</sup> However, if 7-T MRI is more commonly employed in clinical practice, the accuracy and predictability are expected to improve in the future.<sup>9,27</sup> Moreover, it may be possible to measure wall thickness at the same time as PC-MRA,<sup>2</sup> follow-ups including imaging findings of the aneurysm wall and hemodynamic characteristics will be possible. It would be clinically useful in the future if the number of cases could be increased, and the outcome, such as the relationship between  $V_b/V_a$  and the enlargement of aneurysms and rupture rate during follow-up or surgery, are analyzed prospectively.

## CONCLUSIONS

The bleb redness of UIA and  $V_b/V_a$  calculated by PC-MRA showed a significantly high correlation. Thus, in the future, it might be possible to predict the bleb thickness of aneurysms non-invasively before surgery. This could lead to a more detailed preoperative and intraoperative strategy for clipping and coiling, and surgical treatment can probably be performed more safely.

## DECLARATION OF COMPETING INTEREST

This research was supported by JST CREST, Japan (grant number JPMJCR17A1) and JSPS KAKENHI, Japan (grant number JP18K08938). The datasets during and/or analyzed during the current study available from the corresponding author on reasonable request.

## CRedit AUTHORSHIP CONTRIBUTION STATEMENT

**Hiroki Uchikawa:** Conceptualization, Methodology, Formal analysis, Writing - original draft. **Taichi Kin:** Validation, Software, Writing - review & editing, Supervision, Funding acquisition. **Yasuhiro Takeda:** Investigation, Visualization. **Tsukasa Koike:** Investigation, Visualization. **Satoshi Kiyofuji:** Investigation, Visualization. **Satoshi Koizumi:** Investigation, Visualization. **Taketo**

**Shiode:** Investigation, Visualization. **Yuichi Suzuki:** Resources, Supervision. **Satoru Miyawaki:** Writing - review & editing, Resources, Supervision. **Hirofumi Nakatomi:** Writing - review & editing, Resources, Supervision. **Akitake Mukasa:** Writing - review & editing, Supervision. **Nobuhito Saito:** Writing - review & editing, Supervision, Project administration.

## ACKNOWLEDGMENTS

We thank Editage ([www.editage.com](http://www.editage.com)) for English-language editing. We also thank Dr. Kosuke Kashiwabara, Biostatistics Division of The University of Tokyo Hospital, for statistical consultation.

## REFERENCES

- Chen XL, Chen Y, Ma L, et al. Translucent appearance of middle cerebral artery bifurcation aneurysms is risk factor for intraoperative aneurysm rupture during clipping. *World Neurosurg.* 2017;101:149-154.
- Blankena R, Kleinloog R, Verweij BH, et al. Thinner regions of intracranial aneurysm wall correlate with regions of higher wall shear stress: a 7 T MRI study. *AJNR Am J Neuroradiol.* 2016;37:1310-1317.
- Fukazawa K, Ishida F, Umeda Y, et al. Using computational fluid dynamics analysis to characterize local hemodynamic features of middle cerebral artery aneurysm rupture points. *World Neurosurg.* 2015;83:80-86.
- Kadasi LM, Dent WC, Malek AM. Colocalization of thin-walled dome regions with low hemodynamic wall shear stress in unruptured cerebral aneurysms. *J Neurosurg.* 2013;119:172-179.
- Kimura H, Taniguchi M, Hayashi K, et al. Clear detection of thin-walled regions in unruptured cerebral aneurysms by using computational fluid dynamics. *World Neurosurg.* 2019;121:e287-e295.
- Omodaka S, Sugiyama S, Inoue T, et al. Local hemodynamics at the rupture point of cerebral aneurysms determined by computational fluid dynamics analysis. *Cerebrovasc Dis.* 2012;34:121-129.
- Suzuki D, Funamoto K, Sugiyama S, Nakayama T, Hayase T, Tominaga T. Investigation of characteristic hemodynamic parameters indicating thinning and thickening sites of cerebral aneurysms. *J Biomech Sci Eng.* 2015;10:14-000265.
- van Ooij P, Potters WV, Guédon A, et al. Wall shear stress estimated with phase contrast MRI in an in vitro and in vivo intracranial aneurysm. *J Magn Reson Imaging.* 2013;38:876-884.
- van Ooij P, Zwanenburg JJ, Visser F, et al. Quantification and visualization of flow in the circle of Willis: time-resolved three-dimensional phase contrast MRI at 7 T compared with 3 T. *Magn Reson Med.* 2013;69:868-876.
- Nomura S, Kin T, Kunimatsu A, et al. Registration method between phase-contrast magnetic resonance angiography and time-of-flight magnetic resonance angiography—preliminary study. *J Med Imaging Health Inform.* 2021;11:33-39.
- Hoogeveen RM, Bakker CJ, Viergever MA. Limits to the accuracy of vessel diameter measurement in MR angiography. *J Magn Reson Imaging.* 1998;8:1228-1235.
- Gingold RA, Monaghan JJ. Smoothed particle hydrodynamics: theory and application to non-spherical stars. *Monthly Notices Roy Astronomical Soc.* 1977;181:375-389.
- Spearman C. The proof and measurement of association between two things. *Am J Psychol.* 1904;15:72-101.
- Sugiyama SI, Endo H, Omodaka S, et al. Daughter sac formation related to blood inflow jet in an intracranial aneurysm. *World Neurosurg.* 2016;96:396-402.
- Cebral JR, Mut F, Weir J, Putman C. Quantitative characterization of the hemodynamic environment in ruptured and unruptured brain aneurysms. *AJNR Am J Neuroradiol.* 2011;32:145-151.
- Suzuki T, Takao H, Suzuki T, et al. Determining the presence of thin-walled regions at high-pressure areas in unruptured cerebral aneurysms by using computational fluid dynamics. *Neurosurgery.* 2016;79:589-595.
- Sugiyama S, Niizuma K, Nakayama T, et al. Relative residence time prolongation in intracranial aneurysms: a possible association with atherosclerosis. *Neurosurgery.* 2013;73:767-776.
- Meng H, Tutino VM, Xiang J, Siddiqui A. High WSS or low WSS? Complex interactions of hemodynamics with intracranial aneurysm initiation, growth, and rupture: toward a unifying hypothesis. *AJNR Am J Neuroradiol.* 2014;35:1254-1262.
- Szajer J, Ho-Shon K. A comparison of 4D flow MRI-derived wall shear stress with computational fluid dynamics methods for intracranial aneurysms and carotid bifurcations—a review. *Magn Reson Imaging.* 2018;48:62-69.
- Berg P, Vofß S, Saalfeld S, et al. Multiple Aneurysms Anatomy Challenge 2018 (MATCH): phase I: segmentation. *Cardiovasc Eng Technol.* 2018;9:565-581.
- Valen-Sendstad K, Bergersen AW, Shimogonya Y, et al. Real-world variability in the prediction of intracranial aneurysm wall shear stress: the 2015 International Aneurysm CFD Challenge. *Cardiovasc Eng Technol.* 2018;9:544-564.
- Berg P, Saalfeld S, Vofß S, Beuing O, Janiga G. A review on the reliability of hemodynamic modeling in intracranial aneurysms: why computational fluid dynamics alone cannot solve the equation. *Neurosurg Focus.* 2019;47:E15.
- Sugiyama SI, Endo H, Niizuma K, et al. Computational hemodynamic analysis for the diagnosis of atherosclerotic changes in intracranial aneurysms: a proof-of-concept study using 3 cases harboring atherosclerotic and nonatherosclerotic aneurysms simultaneously. *Comput Math Methods Med.* 2016;2016:2386031.
- Kadasi LM, Dent WC, Malek AM. Cerebral aneurysm wall thickness analysis using intraoperative microscopy: effect of size and gender on thin translucent regions. *J Neurointerv Surg.* 2013;5:201-206.
- Uluç K, Kujoth GC, Başkaya MK. Operating microscopes: past, present, and future. *Neurosurg Focus.* 2009;27:E4.
- van Hespren KM, Zwanenburg JJM, Harteveld AA, Luijten PR, Hendrikse J, Kuijff HJ. Intracranial vessel wall magnetic resonance imaging does not allow for accurate and precise wall thickness measurements: an ex vivo study. *Stroke.* 2019;50:e283-e284.
- Kleinloog R, Korkmaz E, Zwanenburg JJ, et al. Visualization of the aneurysm wall: a 7.0-tesla magnetic resonance imaging study. *Neurosurgery.* 2014;75:614-622.

Received 6 October 2020; accepted 5 January 2021

Citation: *World Neurosurg.* X (2021) 10:100098.

<https://doi.org/10.1016/j.wnsx.2021.100098>

Journal homepage: [www.journals.elsevier.com/world-neurosurgery-x](http://www.journals.elsevier.com/world-neurosurgery-x)

Available online: [www.sciencedirect.com](http://www.sciencedirect.com)

2590-1397/© 2021 The Authors. Published by Elsevier Inc.

This is an open access article under the CC BY-NC-ND

license (<http://creativecommons.org/licenses/by-nc-nd/4.0/>).



## SUPPLEMENTAL METHODS

Wall shear stress (WSS) calculation

$$\text{WSS} = \mu |\dot{\gamma}|$$

$$|\dot{\gamma}| = \sqrt{2\mathbf{D} : \mathbf{D}}$$

$$\mathbf{D} = \mathbf{I} / 2 \{ (\nabla \mathbf{u}) + (\nabla \mathbf{u})^t \}$$

$$\nabla \mathbf{u} = \begin{bmatrix} \partial v_x / \partial x & \partial v_y / \partial x & \partial v_z / \partial x \\ \partial v_x / \partial y & \partial v_y / \partial y & \partial v_z / \partial y \\ \partial v_x / \partial z & \partial v_y / \partial z & \partial v_z / \partial z \end{bmatrix}$$

Blood viscosity ( $\mu$ ) was set at  $3.6 \times 10^{-3}$  Pa · s.  $|\dot{\gamma}|$ ,  $\mathbf{D}$ , and  $\nabla \mathbf{u}$  indicate shear rate, deformation rate tensor, and velocity gradient tensor, respectively. In addition,  $v_x$ ,  $v_y$ , and  $v_z$  indicate the velocity in the x, y, and z axes.

## REFERENCE

1. Gotoh H. *Ryushihou [Particle Method]*. Tokyo: Morikita Syuppan; 2018:208-209.